Anomalous temperature dependence of photoinduced fluidity in chalcogenide glasses

D. Th. Kastrissios and G. N. Papatheodorou
Foundation for Research and Technology Hellas, Institute of Chemical Engineering and High Temperature Chemical Processes, P.O. Box 1414, GR-26500 Patras, Greece
and Department of Chemical Engineering, University of Patras, GR-26500 Patras, Greece

S. N. Yannopoulos*
Foundation for Research and Technology Hellas, Institute of Chemical Engineering and High Temperature Chemical Processes, P.O. Box 1414, GR-26500 Patras, Greece

(Received 1 August 2001; revised manuscript received 30 November 2001; published 8 April 2002)

A temperature-dependent, sub-band-gap, light-scattering study of the vibrational modes of vitreous As_2S_3 fibers during the photoinduced fluidity effect is reported. The structural changes that give rise to the effect are detected mainly through variations in the degree of polarization of the scattered light. The results show a nonmonotonic behavior in the observed structural changes interpreted as a reduction in the flow ability of the glass a few degrees above room temperature followed by a subsequent increased ability to plastic deformation at higher temperatures, but still well below the glass-transition temperature. Studies on the nonstoichiometric concentration $As_{25}S_{75}$ at room temperature revealed noticeable differences with arsenic trisulfide. The relation between the illuminating energy and the band gap of the glass has also been investigated. An account for the possible nature of these experimental facts is attempted in terms of the specific structural units constituting the glass structure.

DOI: 10.1103/PhysRevB.65.165211 PACS number(s): 42.70.Gi, 78.30.−j

I. INTRODUCTION

The issue concerning the flow or plastic deformation of solids without heat provision has been recently addressed in the case of an amorphous semiconductor.[1] It was demonstrated that fluidity enhancement of a chalcogenide glass can be obtained in a purely athermal way, i.e. by illuminating the glass with light having energy smaller than the band gap of the semiconductor. In particular, athermal increase of the chalcogenide-glass network fluidity due to the simultaneous effect of (i) sub-band-gap light illumination and (ii) application of an external mechanical stress was evidenced through the increasing length of a vitreous As_2S_3 (ν-As_2S_3) fiber. This was interpreted as the result of specific structural transformations occurring at the illuminated point. The photoelectronic or athermal origin of this effect, that has been called *photoinduced fluidity*, can be evidenced through the unexpected temperature dependence it exhibits.[1] Specifically, while ordinary flow of glass-forming liquids follows either strong or mild temperature dependence, being always facilitated when the temperature of the material increases,[2] it was observed that photoinduced fluidity is hindered at elevated temperatures. This was manifested in the considerable suppression of the material's ability to flow or to plastically deform at the illuminated point as the temperature increased.[1] It has been pointed out in Ref. 1 that both *intramolecular* and *intermolecular* photoinduced structural mechanisms might be possibly involved; although their distinct role was not specified.

Photoinduced structural changes occur in amorphous chalcogenide semiconductors when they are illuminated by band-gap or sub-band-gap light. The absorption of light results in the creation of electron-hole (*e-h*) pairs (excitons), whose subsequent recombination leads to structural changes eventually through bond reforming processes. Whereas various effects, emerging from such structural changes such as photodarkening (redshift in the optical absorption edge), photoinduced anisotropy, volume photoexpansion, and athermal photomelting at low temperatures, to name a few, have been extensively studied and understood to a good extent,[3] the reported photoinduced fluidity effect has received less attention up until now.

There exist few works so far aimed at elucidating the microscopic origin of the photoinduced fluidity effect. Fritzsche has tried[4] to account for the athermal fluidity enhancement through the well-known, self-trapped exciton model.[5] According to this idea some of the photoexcited (*e-h*) pairs may recombine nonradiatively through an intermediate transient state. The final recombination may yield a bonding arrangement orthogonal to the initial configuration and the observed macroscopic change in the fluidity can be considered as the cumulative effect of these local configuration changes. First-principles molecular-dynamics simulations used to calculate light-induced structural changes and diffusive motion in a chalcogenide glass (As_2Se_3) revealed a diffusive motion characterized by short time scale. This finding was interpreted as the initial stage of the athermal photoinduced fluidity.[6]

From the experimental point of view, Raman spectroscopy has been used to study both the low-energy excitations and high-frequency optical modes of ν-As_2S_3 during the photoinduced fluidity effect at room temperature.[7,8] Preliminary data on the temperature dependence of the photoinduced fluidity effect have also been reported in Ref. 9. The aim of the present work is twofold. First, to present a detailed temperature-dependence Raman spectroscopic study in order to monitor the specific spectral features associated with the anomalous temperature dependence of the photoen-

hanced fluidity originally observed by Hisakuni and Tanaka.[1] Second, apart from the As_2S_3 (or $As_{40}S_{60}$) stoichiometric concentration that forms a layerlike structure,[3] we have also included in our study the nonstoichiometric compound $As_{25}S_{75}$. The latter is characterized by a more flexible structure than to the $As_{40}S_{60}$, having also a wider band gap that will allow us to check the role of the incident energy on the strength of the photoinduced fluidity effect by choosing different illuminating sources.

The paper is arranged as follows. Section II contains a brief description of the experimental details, i.e., fiber preparation and light-scattering apparatus. In Sec. III the results are presented. Section IV contains their discussion focusing on the temperature dependence of the depolarization ratio vs stress curves, the difference in the structure between the two glasses studied in this work, and the degree of depolarization of the individual vibrational lines in the high frequency region. Finally, the most important conclusions drawn from the present study are summarized in Sec. V.

II. EXPERIMENT

ν-As_2S_3 fibers have been obtained through rapid extraction of tiny quantities from the melt at about 600 °C. The obtained fibers had diameters in the range 90–280 μm. The diameters were found to be constant for lengths much longer than those used in our experiment ($\sim$5 cm). A homemade stretching microdevice has been devised that can—in a controllable way—provide the desired elongation stress to the attached fiber as described elsewhere.[7,8] Typical values for the applied stress fall within the range 0×10^7 to 24×10^7 dyn cm^{-2}. A specially constructed heating mantle has been adapted to the stretching device in such a way so as to provide the required heat to the fiber. Great care was taken to avoid any undesired heating to the stress-providing spring that could change its precalibrated force constant. Therefore, temperatures as high as 160 °C could be reached at the fiber's location while keeping the spring at room temperature.

The 647.1-nm ($E^{\rm ill}\approx1.92$ eV) and 514.5-nm ($E^{\rm ill}\approx2.41$ eV) lines emerging from Kr^+ and Ar^+ lasers (spectra physics), respectively, were used to induce the photostructural changes to the systems studied. At the same time the right-angle scattered light was collected and analyzed by a double monochromator with a resolution fixed at 1.5 cm^{-1} during all measurements. The laser power was set at a level low enough (10 W cm^{-2} on the fiber) so as to avoid thermal effects due to laser heating. Both VV (vertical-vertical) and HV (horizontal-vertical) scattering geometries were employed, while the fiber was kept always perpendicular to the scattering plane. The signal after its detection from a water-cooled photomultiplier and its amplification from standard electronic equipment was transferred to a computer. Details concerning the experimental procedure can be found elsewhere.[7,8]

III. RESULTS

Before proceeding to the presentation and the discussion of the results obtained in the present work, it would be helpful to briefly mention the most important facts emerged from the previous room-temperature studies.[7,8] It was shown that the main changes detected in the Raman spectra as a function of the external stress are related to changes in the scattered-intensity depolarization ratio $\rho(\omega)$. The systematic variations in $\rho(\omega)$ with the magnitude of the external stress were considered as an indicator of the photoinduced fluidity effect; this was based on the observation that no detectable changes are discerned from the measured spectra, i.e., $\rho(\omega)$ remains constant independent of the exposure time, if no stress is applied. Thus, the changes observed in the depolarization ratio are due to the *combined* effect of illumination and the application of the external stress. This implies that illumination alone does not engender fluidity; it rather brings the structure to a state amenable to flow or to plastically deform with the aid of an external mechanical stimulus. Therefore, the whole effect could also be conceived as a kind of *photoinduced ductility*. Summarizing, what became clear from the room-temperature study is that the monotonic-sigmoid increase of the depolarization ratio vs stress is a systematic indicator of the structural changes occurring during the combined stretching/illuminating effect.

As mentioned in the introduction, Hisakuni and Tanaka studied the temperature dependence of the photoinduced fluidity and found that the effect became less appreciable at higher temperatures. In particular, they calculated the fluidity up to the temperature $\sim$50 °C and found an Arrhenius increase of almost one order of magnitude in an interval of about 40 °C. In the present work, we have recorded Raman spectra in the temperature interval 20–120 °C, thus extending the information over a region much higher than that used in Ref. 1. The Stokes side of the high-frequency Raman spectra of ν-As_2S_3 fibers at four different temperatures as a function of the applied stress are shown in Fig. 1. The low-frequency region has also been registered but will not be the subject of the present work. Extensive treatment concerning the stress dependence of the low-energy excitations can be found elsewhere.[8]

The most obvious observation from Fig. 1 is that the main changes taking place in each set of spectra pertain to a monotonic and more rapid increase of the depolarized spectrum compared to the polarized one. This is better discerned by following the changes of the isotropic (ISO) component of the spectrum defined as $I^{\rm ISO}=I^{\rm VV}-(4/3)I^{\rm HV}$, which is plotted in Fig. 1 as a dotted line alongside with the polarized and depolarized intensities. It should be reminded that the isotropic part of the Raman spectrum arises from the diagonal elements of the polarizibality tensor and therefore reveals information related to the symmetry properties of the vibrational modes. Similar changes in the spectra were also observed in the room-temperature, light-scattering study of ν-As_2S_3.[7,8]

However, what interestingly emerges from the temperature-dependence study is that the rate of increase of the depolarization ratio is not constant, even nonmonotonic, as a function of the temperature, as can be seen from Fig. 1. To quantify these changes we have followed a procedure similar to that described elsewhere.[8] In particular, three Gaussian lines were used to fit the 260–430 cm^{-1} frequency

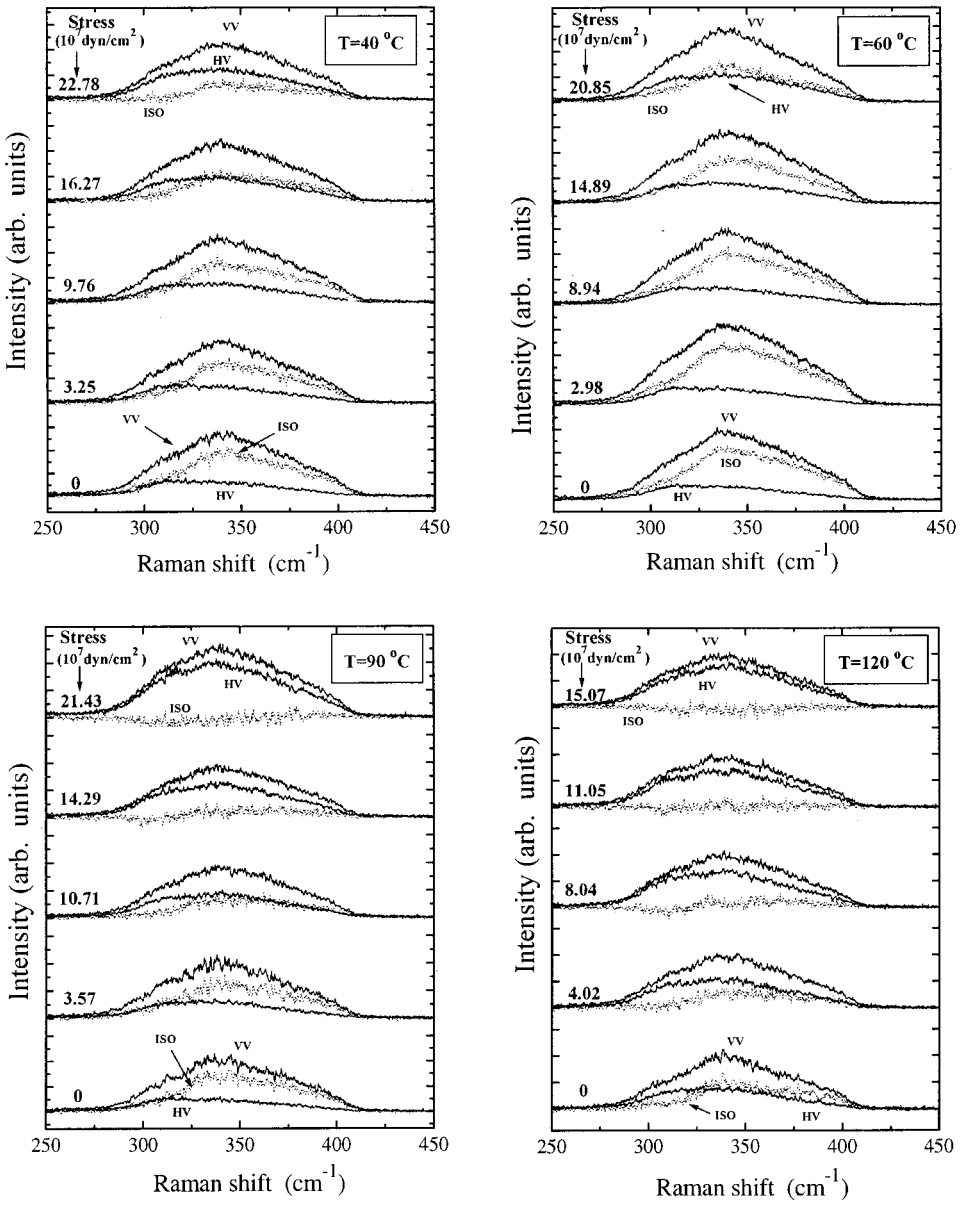

FIG. 1. Representative high-frequency Stokes-side Raman spectra of ν-As_2S_3 fibers under external elongation stress at 40, 60, 90, and 120 °C. Both polarization geometries, VV and HV, are shown alongside with the purely isotropic spectra (dotted line) that are determined as described in the text. The magnitude of stress applied is given in terms of 10^7 dyn cm^{-2}.

region for both the polarized and the depolarized spectra. The depolarization ratios of the 260–430 cm^{-1} area calculated either from the fit or by integration were found almost equal. These ratios are presented in Fig. 2 as a function of the applied stress at the four measured temperatures. We observe that at 40 °C the sigmoid curve, representing the depolarization-ratio increase, reaches a plateau that hardly exceeds the half of the corresponding plateau value of the room-temperature curve. Subsequent temperature rise, up to 60 °C, renders the effect even less appreciable. In other words, structural reorganization during the photoinduced fluidity effect seems to be hindered at higher temperature.

Up to this point, the temperature dependence of the depolarization ratio is reminiscent to the temperature dependence of the photoinduced fluidity data.[1] This is a further support to the idea that the depolarization-ratio changes can indeed be related with the photoinduced fluidity effect. Hisakuni and Tanaka[1] managed to calculate the viscosity of the glass, induced by light illumination, relating the viscous strain rate with the applied stress. Their data demonstrated that the photoinduced fluidity decreases by almost one order of magnitude in an interval of 40 °C, however, being always many orders of magnitude higher than the fluidity of the ''dark'' (not illuminated) sample.

This picture changes drastically when the measurements are extended over a wider temperature range than that of Ref. 1. Indeed, it is evident from Fig. 2 that the depolarization ratio (and presumably the fluidity) increases again as is seen at the 90 °C data, which eventually coincide with those of the room-temperature study. A further increase of the temperature to 120 °C leads to more noticeable changes of $\rho(\omega)$ even at low values of the applied stress. Bearing in mind that the glass-transition temperature of the material, $T_g \approx 210$ °C,[10] is still well above the highest employed temperature in our experiment, it seems highly unlikely that a substantial softening of the glass structure at 120 °C takes place. In fact, even at the temperature of 120 °C the ''dark'' viscosity of As_2S_3 is two or three orders of magnitude higher

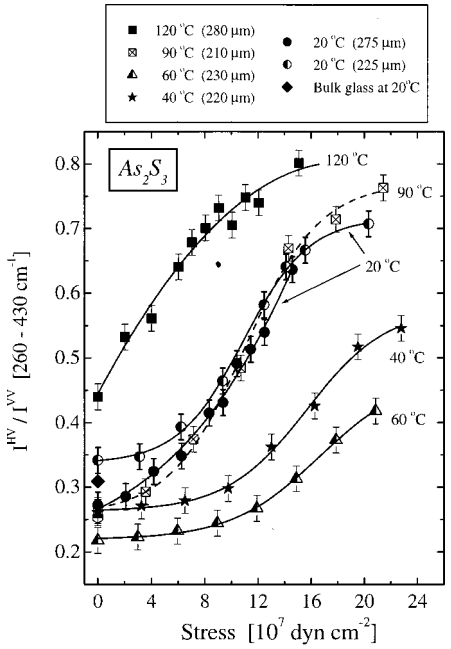

FIG. 2. Stress dependence of the area depolarization ratio in the region 260–430 cm^{-1} as a function of the externally applied stress for $As_{40}S_{60}$ at the temperatures: 20 °C (filled and semi-filled circles), 40 °C (stars), 60 °C (semifilled triangles), 90 °C (crossed squares), and 120 °C (filled squares). The diameter of the fiber employed in each case is also given on top of the figure.

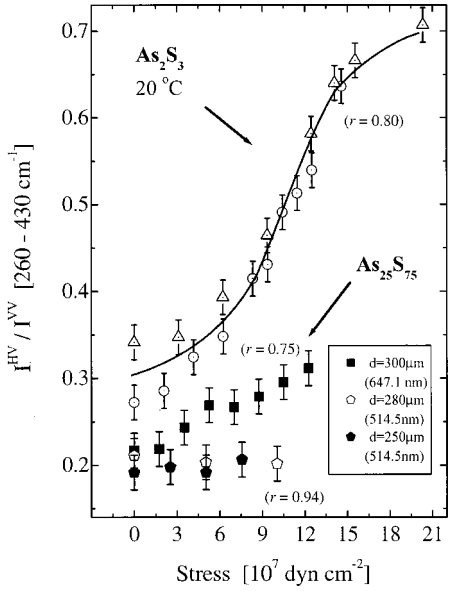

FIG. 3. Stress dependence of the area depolarization ratio in the region 260–430 cm^{-1} as a function of the externally applied stress for $As_{25}S_{75}$ at room temperature (filled squares). The room temperature data of $As_{40}S_{60}$ are also shown for comparison. Empty and filled diamonds represent the data for $As_{25}S_{75}$ recorded with the 514.5-nm laser line.

than the viscosity at T_g and therefore thermal softening of the glass structure is not expected to intervene.

To affirm that temperature does not play a ''direct'' role, that is we have no thermal structure softening at the highest temperature reached in the present work, the following experiment was performed. A fiber was stressed at 120 °C for 3 h without being illuminated at a stress magnitude of about 8×10^7 dyn cm^{-1}. Then, the fiber was cooled down to room temperature and the depolarization ratio was found to be ~0.23, only 0.04 higher than the corresponding value before the thermal treatment. We may, therefore, conclude that the combined effect of temperature (at least up to the value 120 °C used in this work) and stress, without illumination, does not cause any structural changes. Thus, the features illustrated in Fig. 2 are indeed photoinduced.

So far, the studies on the athermal photoinduced fluidity effect have been concentrated only on the stoichiometric composition As_2S_3 or $As_{40}S_{60}$.[1,7,8] To examine if the effect is quite general, studies on other chalcogenides or even other concentrations of the As_xS_{100-x} glass-forming family have to be performed. The latter is an interesting case since one can almost smoothly pass (by reducing x) from the layerlike structure ($x=40$) to the more flexible arrangement containing the chainlike or ringlike fragments characteristic of sulfur-rich mixtures. For this, we have chosen to study the $As_{25}S_{75}$ glass whose structure is less rigid compared with the stoichiometric one due to the lower mean coordination number per atom. The room-temperature results for the $As_{25}S_{75}$ composition are shown in Fig. 3 as solids squares. It is clearly seen that the effect on the depolarization ratio and hence on the photoinduced fluidity is much weaker compared to the room-temperature data of $As_{40}S_{60}$. The $As_{25}S_{75}$ glass has a wider band gap than the stoichiometric glass, $E_g=2.55$ eV,[11] and therefore the 514.5-nm (2.41 eV) laser line can also be used as a sub-band-gap illuminating source. The depolarization ratio as a function of the applied stress for the $As_{25}S_{75}$ concentration measured with the 514.5-nm laser line are shown in Fig. 3 as open and solid diamonds for two different runs of the experiment. These data show the obvious ineffectiveness of the 514.5-nm laser line, which lies below but very close to the band gap of the glass, to produce such structural changes that could result in the plastic deformation of the fiber. This will be discussed in the following section.

Before proceeding to the discussion of the above results, we have to stress two particular points. First, one could argue that the preparation procedure might induce some ordering in the fiber due to its rapid extraction of the melt. The depolarization ratio (which is sensitive to such ordering effects) of the unstressed fiber and the bulk glass are found to be equal within experimental error. This implies that the structure of the fiber is still homogeneous and indistinguishable from the structure of the bulk glass. Second, changes in the fiber diameter, including photoinduced expansion of the unstressed or slightly stressed fiber and subsequent contraction in the diameter due to the applied stress, are not expected to influence the nonmonotonic temperature behavior of Fig. 2. This stems from the fact that the depolarization ratio is the ratio between two scattered intensities and therefore the dependence on the incident number of photons, inducing the effect, is eliminated.

IV. DISCUSSION

A. As_2S_3: Temperature dependence of the $\rho(\omega)$ vs stress curves

Having established a link between the photoinduced fluidity effect and the monotonic increase of the Raman-scattered intensity depolarization ratio, at a particular temperature, the following observations emerge from Fig. 2. The rise of temperature at least up to 60 °C causes a hindrance in the flow process, as was also demonstrated in the work by Hisakuni and Tanaka. This finding supports the athermal character of the effect and could be rationalized by considering that the geminate recombination rate of the photoexcited *e-h* pair is reduced with increasing temperature.[1] It is expected that geminate recombination, i.e., recombination of the same (*e-h*) pair that has been previously created, results in the atomic bond transformation that contribute to the flow facilitation under the application of external stress. Bearing in mind that rise of temperature monotonically reduces the geminate recombination rate,[3] due to diffusion of the excited (*e-h*) carriers apart from each other, a plausible explanation is provided to account for the decrease of the photoexcited flow ability at 40 and 60 °C.

The aforementioned picture changes drastically when the study of the vibrational modes is performed at higher temperatures. As it was actually shown in Fig. 2 the data concerning the stress dependence of the depolarization ratio at 90 °C are almost indistinguishable from the corresponding room-temperature data. Since the influence of temperature on the geminate recombination rate is monotonic, we have to reckon on another factor determining the structural changes observed at elevated temperatures. We had considered in the room-temperature study[8] that the ''orientation'' of bonds along the stressing direction might arise from changes either in local atomic configuration and/or by layer unfolding processes like those specified in the buckling model.[12] This model is based on the widely adopted idea that particular chalcogenides, such as the stoichiometric As_2S_3 glass, retain to some degree the layered structure of its parent crystal, thus containing two types of bonds, i.e., strong covalent ones within the layer and weak van der Waals bonds between the layers. The covalent bonds are responsible for the glass structure integrity of the chalcogenide layers and other properties such as the glass-transition temperature and are affected by temperature only close and above T_g. On the other hand, the sublattice of the weak bonds is the one that contains the entities that are easily responsive to incident light and is ultimately responsible for the photoinduced phenomena. Due to the smaller energy barriers that are involved in this case, weak-bond restructuring may occur even at temperatures much lower than T_g.

Studies on the temperature dependence (from room temperature to above T_g) of the x-ray structure factor of As_xS_{100-x} glasses have revealed an unexpected increase in the first sharp diffraction peak intensity with increasing temperature, while the second diffraction peak intensity normally decreased.[13] These finding have been interpreted as evidence of an increasing layering with temperature. This may occur since, as the temperature rises, the thermal energy provided may allow the atoms to relax their strained bonding arrangement rendering the layer smoother.

The aforementioned data offer a possibility to explain the anomalous behavior of the photoinduced fluidity observed through the Raman depolarization ratio. Indeed, the nonmonotonic dependence on temperature of the $\rho(\omega)$ curves shown in Fig. 2 may arise from the competition of two opposing effects. The first is the decreasing geminate recombination rate, discussed previously, which is considered to persist over the whole temperature range scanned in the present work. On the other hand, ordering effects, viz, enhanced layering, have an opposite trend compared to the previous mechanism, tending to facilitate the plastic deformation imposed by the external stress. The reversal of the fluidity vs temperature curve occurring above 60 °C implies the predominance of the second mechanism, that is, layer ordering. The enhancement of layer ordering is presumably the origin of the increased zero-stress $\rho(\omega)$ value at 120 °C (Fig. 2).

Finally, one could argue that the band-gap lowering due to the temperature rise up to 120 °C might have some impact on the observed behavior of the depolarization ratio. The band-gap change between room temperature and 120 °C is estimated to be $\Delta E_g \approx 0.072$ eV [$E_g(20\,°\mathrm{C}) \approx 2.409$ eV and $E_g(120\,°\mathrm{C}) \approx 2.337$ eV, calculated from the data given in Ref. 14]. Therefore, the 3% lowering of the band gap is not expected to have strong influence on the photoinduced fluidity effect. This is further supported by the fact that the band gap decreases monotonically with increasing temperature, while the observed changes in the depolarization ratio are nonmonotonic.

B. Photoinduced fluidity for the nonstoichiometric $As_{25}S_{75}$ glass

The study of the structural changes during the photoinduced fluidity effect for the $As_{25}S_{75}$ glass, revealed (Fig. 3) that these changes are less significant than the respective ones in the stoichiometric composition ($As_{40}S_{60}$). In the following, we will discuss three possible factors that might contribute to the different properties of the $\rho(\omega)$ vs stress room-temperature curves between the $As_{40}S_{60}$ and $As_{25}S_{75}$ glasses, viz. (i) the difference in their structure, (ii) the relation between incident light energy and band gap, and (iii) the role of the glass-transition temperature.

(i) It is well established that increasing the sulfur content in the As_xS_{100-x} glass family above the stoichiometric point ($1-x=60$) one can in a controllable way modify the structure and hence the rigidity of the glass. In particular, in sulfur-rich glasses the quasi-two-dimensional layers are partially disrupted and chainlike fragments and/or eight-membered sulfur rings are the main structural units.[15] Vibrational spectroscopy has shown that S_8 molecules are present in the sulfur-rich glasses up to $x=35$.[16] It is evident from Fig. 3 that the ordering effects accompanying photoinduced fluidity are less prominent in the case of the less rigid structure. This seems reasonable in the framework of the buckling model. Indeed, the reduction of the layered fragments with increasing sulfur, softens the structure considerably and reduces also its ability to respond to the external stress. This

TABLE I. Ratio r of the illumination light energy to the band gap of the glass. The numbers in parentheses indicate the glass-transition temperature taken from Ref. 10.

Laser line (nm)	$As_{40}S_{60}$ (210 °C)	$As_{25}S_{75}$ (140 °C)
514.5	1.00	0.94
647.1	0.80	0.75

may be envisaged in two different ways. First, the chainlike sulfur configurations could be entangled, thus hindering the flow process. Second, the quasi-one-dimensional character of the chainlike fragments offers the possibility of new relaxation pathways, during illumination, in directions perpendicular to that of the applied stress; such processes are not expected to contribute to orientation enhancement. Both the above mechanisms cannot be realized in the case of two-dimensional layers. Proceeding one step further, we could add here that the photoinduced fluidity effect is expected to be not so prominent also in the case of glasses with three-dimensional network structures since the compact form of the structure and the lack of the weak van der Waals bonds would impede the flow process. It seems that the particular structural softness of the layered materials maximizes the possibility of structural changes that lead to the plastic deformation (flow) of the material.

(ii) Another possible source for the difference in the $\rho(\omega)$ vs stress curves at room temperature for the two studied glasses could be the effectiveness of the light inducing the structural changes or equivalently the relation of the illuminating light energy to the band-gap energy. The modification of the glass structure by increasing the sulfur content increases the band gap of the material changing also the ratio of the illuminating light energy to the band-gap energy. The values of the ratio $r=E^{\mathrm{ill}}/E_g$ for the materials and the laser lines used in the present work are given in Table I. For $r=1.00$ (that is, illumination of $As_{40}S_{60}$ with the 514.5-nm laser line) it was not possible to perform any light-scattering experiment due to strong absorption/heating conditions. A wavelength dependence could be realized only for the $As_{25}S_{75}$ glass. The fact that the structural changes for this glass ($r=0.75$ or 647.1 nm) are less important than the respective for the $As_{40}S_{60}$ glass ($r=0.80$) is not likely to be due to their difference in r. Actually, the two r values are comparable and the penetration of the 647.1-nm laser line in the case of $As_{25}S_{75}$ ($r=0.75$) is even better than the penetration of the same wavelength for the $As_{40}S_{60}$ ($r=0.80$) glass. Let us see now what is the impact of different wavelengths to the same structure. As it is obvious from the data of Fig. 3, when the illumination is performed with near-band-gap light ($r=0.94$) the structural changes leading to photoinduced fluidity are minimal and not detectable. This is quite plausible for the reason that although the efficiency of light in producing excitons is higher with near-band-gap light, the effect occurs only on the surface due to strong absorption, resulting in a vanishing penetration depth and as a consequence elongation of the fiber cannot occur.

(iii) The glass-transition temperature is another factor that has to be taken into account to elucidate the difference of the room-temperature data (647.1 nm wavelength) shown in Fig. 3. The significant role of T_g has been demonstrated in Ref. 13 where the temperature dependence of the first sharp diffraction peak intensity was found to follow a master curve in a T_g-scaled plot for different glasses in the As_xS_{100-x} family. Thus, a direct comparison between the room-temperature data for $As_{40}S_{60}$ and $As_{25}S_{75}$ may be not so informative and a comparison should be instead done at T_g-scaled or reduced temperatures, $\tau=T^{\mathrm{expt}}/T_g$. The 20 °C data for $As_{25}S_{75}$ ($T_g\approx 140\,^{\circ}\mathrm{C}$) correspond to $\tau\approx 0.71$. The τ ratio assumes the same value $\tau\approx 0.71$ in the case of the $As_{40}S_{60}$ glass ($T_g\approx 210\,^{\circ}\mathrm{C}$) for $T^{\mathrm{expt}}\approx 70\,^{\circ}\mathrm{C}$ implying that the room-temperature $\rho(\omega)$ data of $As_{25}S_{75}$ glass should be compared to the 70 °C data of $As_{40}S_{60}$. The closest available data set of $As_{40}S_{60}$ is that of the 60 °C, which interestingly is located very close to the room temperature $\rho(\omega)$ of the $As_{25}S_{75}$ glass. This finding allows us to adopt the idea that structural changes accompanying photoinduced fluidity might be governed by glass-transition dynamics. If the above hypothesis is correct, then the photoinduced fluidity effect for the $As_{25}S_{75}$ glass is not less prominent compared to that observed for the stoichiometric composition. Measurements of this glass ($As_{25}S_{75}$) at $T\approx -20\,^{\circ}\mathrm{C}$ would result in a $\rho(\omega)$ vs stress curve similar to the room-temperature curve of $As_{40}S_{60}$, if glass transition dynamics do indeed rule photoinduced fluidity.

C. Individual depolarization ratios of the high-frequency vibrational modes

Up until now, we have treated the high-frequency intramolecular vibrations of $As_{40}S_{60}$ as a whole without focusing on the spectral features of the individual bands forming the 260–430 cm^{-1} spectral envelope. We should remind here that according to a ''molecular model'' analysis[17] the above region contains three vibrational modes; the ν_1 and ν_3 vibrational modes of the AsS_3 pyramidal unit ($C_{3\nu}$ symmetry) at 342 and 310 cm^{-1} respectively, and the ν_3' vibrational mode of the waterlike As-S-As unit ($C_{2\nu}$ symmetry) at 392 cm^{-1}. A more detailed examination of the band shapes in this frequency region reveals significant systematic changes as a function of the applied stress for all temperatures studied. In particular, the three peaks ν_1, ν_3, and ν_3' exhibit a clear difference in the degree of modification of $\rho(\omega)$ as a function of the applied stress. Analyzing the spectral envelope 260–430 cm^{-1} with a set of three Gaussian peaks, we were able to track the changes in $\rho(\omega)$ for each peak. These individual depolarization ratios have been normalized to the zero-stress value in order to reveal their relative changes and are plotted in Fig. 4 for all temperatures studied in the present work. It is evident that the increase of the ν_3' peak plays the dominant role in all cases. This particular vibrational mode corresponds to the interplay of the polarizability ellipsoid of the waterlike AsS_2-S-AsS_2 unit between two orientations, however, maintaining unchanged the magnitude of the polarizability ellipsoid,[18] see Fig. 5(a). Therefore, the fact that this particular vibrational mode is the most amenable to the

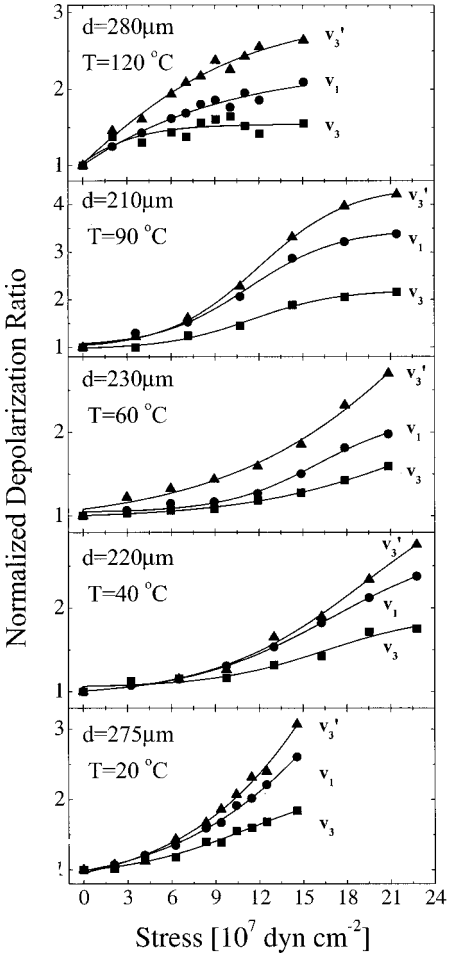

FIG. 4. Normalized depolarization ratio in the region 260–430 cm^{-1} as a function of the externally applied stress. At all temperatures shown the ν_3' peak, as described in the text, exhibits the more drastic changes. Solid lines are guides to the eye.

stress-illumination process is not irrational, and can be accounted for by the simplistic sketch of Fig. 5(b) describing the layer flattening as a result of light illumination and the application of the mechanical stress. The disposition of the composite waterlike AsS_2-S-AsS_2 molecule in a less ruffled layer [sketch (ii)] changes also the orientation of the polarizability ellipsoids that can finally lead to the behavior observed in Fig. 4.

V. CONCLUDING REMARKS

In the present work, we have undertaken an inelastic light-(Raman-) scattering investigation of the vibrational modes during the evolution of the photoinduced fluidity effect for the $As_{40}S_{60}$ and $As_{25}S_{75}$ chalcogenide glasses. Changes in the depolarization ratio for the former one have been investigated at different temperatures (always below T_g), while for the latter the incident-light-energy dependence has been examined. The main conclusions drawn from the present work can be summarized as follows.

The temperature dependence of the Raman depolarization ratio follows the trend observed by Hisakuni and Tanaka up

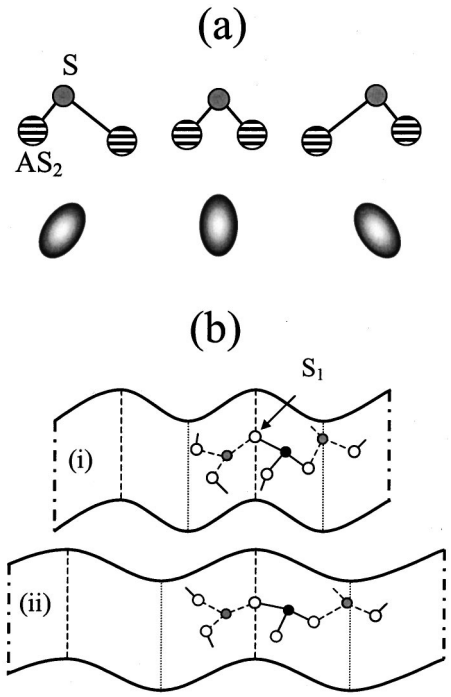

FIG. 5. (a) Schematic representation of the ν_3' vibrational mode corresponding to the waterlike AsS_2-S_1-AsS_2 unit. (b) Idealistic sketch of the layer flattening during the athermal photoinduced fluidity effect: (i) layer before stretching, (ii) layer after stretching. S_1 denotes the central sulfur atom of the AsS_2-S_1-AsS_2 unit.

to 60 °C, i.e., a decreasing ability to plastic deformation or flow was observed with increasing temperature. This behavior was reversed at higher temperatures where ordering effects start to become significant. This nonmonotonic temperature dependence of the structural changes during the photoinduced fluidity effect has been rationalized by invoking the competition between two opposing effects. These are (a) the decreasing geminate recombination rate with increasing temperature that impedes photoinduced fluidity and (b) layer unfolding processes at higher temperatures that dominate above ~60 °C.

The magnitude of the photoinduced fluidity in the case of a ''softer'' or more flexible structure ($As_{25}S_{75}$) was found to be considerably less than the corresponding one of the stoichiometric ($As_{40}S_{60}$) glass, both measured at room temperature. Arguments have been presented to account for this effect based on either the reduced ability of the soft structure in response to the external mechanical stimulus or the fact that T_g-scaled data should be compared. In the latter case $As_{40}S_{60}$ and $As_{25}S_{75}$ exhibit comparable photoinduced fluidity behavior at the same T_g-scaled or reduced temperature. The illumination energy dependence of the effect for $As_{25}S_{75}$ showed that near-band-gap light although more effective in $(e\text{-}h)$ pair creation results in no detectable structural changes related to fiber elongation, since it acts only on the surface of the fiber due to high absorption conditions.

A close examination of the individual depolarization ratios of the high-frequency vibrational modes in $As_{40}S_{60}$ has revealed that the vibrational mode related to the interpyramidal connection is systematically more sensitive to the

illumination/stress effect. Layer flattening process might be possibly involved to this finding.

In conclusion, what emanates from the present study is that the anomalous temperature dependence of the photoenhanced fluidity is a photoelectronic process that belongs to a general class of light-induced, phase changing phenomena such as photocrystallization,[3] photoamorphization,[19] and photomelting[20] as well as reversible nanocontraction and dilation in thin amorphous $As_{50}Se_{50}$ films induced by polarized light.[21] Further, the recently reported effect of optical field-induced mass transport[22] by band-gap excitation in As_2S_3 glass and the concomitant formation of giant relief modulations seems to be closely related with the photoenhanced flow process on which the present study focuses.

*Corresponding author. Email address: sny@iceht.forth.gr

[1] H. Hisakuni and K. Tanaka, Science **270**, 974 (1995).

[2] L.-M. Martinez and C. A. Angell, Nature (London) **410**, 663 (2001).

[3] For general reviews on the subject see: (a) A. V. Kolobov, and K. Tanaka, in *Handbook of Advanced Electronic and Photonic Materials and Devices*, edited by H. S. Nalwa, (Academic, New York, 2001), Vol. 5, pp. 47–90; (b) K. Shimakawa, A. V. Kolobov, and S. R. Elliott, Adv. Phys. **44**, 475 (1995).

[4] H. Fritzsche, Solid State Commun. **99**, 153 (1996).

[5] H. Fritzsche, Philos. Mag. B **68**, 561 (1993).

[6] J. Li and D. A. Drabold, Phys. Rev. Lett. **85**, 2785 (2000).

[7] D. T. Kastrissios, S. N. Yannopoulos, and G. N. Papatheodorou, Physica B **296**, 216 (2001).

[8] D. T. Kastrissios, G. N. Papatheodorou, and S. N. Yannopoulos, Phys. Rev. B **64**, 214203 (2001).

[9] D. T. Kastrissios and S. N. Yannopoulos, *Proceedings of the 19th International Conference on Amorphous Semiconductors—Science and Technology (ICAMS19), Nice, France, 2001* [J. Non-Cryst. Solids (to be published)].

[10] For a recent experimental determination of the glass-transition temperature see, T. Wagner, S. O. Kasap, M. Vlcek, A. Sklenar, and A. Stronski, J. Non-Cryst. Solids **227-230**, 752 (1998).

[11] K. Matsuishi, R. Arima, K. Kagota, and S. Onari, J. Non-Cryst. Solids **266-269**, 938 (2000); in this work the authors provide the E_g values for the concentration $x=20$ and $x=30$, we have therefore estimated the E_g for the $x=25$ glass assuming a linear relation between $x=20$ and $x=30$.

[12] J. Ihm, J. Phys. C **18**, 4741 (1985).

[13] L. E. Busse, Phys. Rev. B **29**, 3639 (1984).

[14] H. Tichá, L. Tichý, P. Nagels, E. Sleeckx, and R. Callaerts, J. Phys. Chem. Solids **61**, 545 (2000).

[15] A. Feltz, *Amorphous Inorganic Materials and Glasses* (VCH, Weinheim, 1993).

[16] R. J. S. Ewen, M. J. Sik, and A. E. Owen, Solid State Commun. **33**, 1067 (1980).

[17] G. Lucovsky and R. M. Martin, J. Non-Cryst. Solids **8-10**, 185 (1972).

[18] K. Nakamoto, *Infrared and Raman Spectra of Inorganic and Coordination Compounds* (Wiley-Interscience, New York, 1986).

[19] A. V. Kolobov and S. R. Elliott, J. Non-Cryst. Solids **189**, 297 (1995).

[20] V. V. Poborchii, A. V. Kolobov, and K. Tanaka, Appl. Phys. Lett. **74**, 215 (1999).

[21] P. Krecmer, A. M. Moulin, R. J. Stephenson, T. Rayment, M. E. Welland, and S. R. Elliott, Science **277**, 1799 (1997).

[22] A. Saliminia, T. V. Galstian, and A. Villeneuve, Phys. Rev. Lett. **85**, 4112 (2000).